Circular Prediction Algorithms – Hybrid Filters

Dirk Tenne [*] Tarunraj Singh [†]

Abstract

The focus of this paper is on the development of a geometric algorithm as an alternative to the coordinated turn procedures. The fact that the trajectories of maneuvering targets are always smooth, has been exploited to derive an algorithms, which constrains the predicted position of the target to lie on a circle formed by prior measurements. This filter is then used in conjunction with an α-β filter to arrive at a series of filters which are tested on benchmark trajectories. The performances show promising results for the proposed filters.

Keywords: Target tracking, circular prediction, hybrid filter

1 Introduction

The estimation and prediction of the kinematics of a dynamic object requires the use of a dynamic model and discrete time data. A majority of target trackers are based on a straight line maneuver, where model uncertainties and man-made disturbances are accounted for as stochastic acceleration. On the contrary, complex non-linear models have been developed to capture the real object dynamics. These models are applied to special maneuvers such as the coordinated turn. The focus of this paper is on the development of an algorithm constraining the predicted state to a circular turn.

Filters based on a constant velocity or constant acceleration trajectory are implemented as α-β [1, 2, 3], α-β-γ [4, 5] and linear Kalman filters [6, 7, 8]. Singer [9] developed an acceleration model for manned maneuvering targets with exponentially autocorrelated acceleration. He viewed this acceleration as perturbations upon the constant velocity trajectory. Relaxing the straight line assumption, Berg [10] augmented Singer‘s model by an "adaptive estimation of the mean target jerk", which is the result of a coordinated turn. The coordinated turn is a special maneuver, which is consistent with the bank-to-turn flight characteristics of a fixed-wing aircraft [11]. This planar maneuver is defined by assuming:

- the aerodynamic lift (L) and the resulting thrust (T) are constant
- the roll rate (p) is zero

This algorithm is based on aircraft related parameters like thrust, lift and target inertial angular velocity components (p, q, r), which form a set of coupled non-linear differential equations. Bishop and Antoulas [12, 13] treated the aircraft as a material point as a result of assuming the angle of attack (α_x) and sideslip (β) to be zero. In combination with the coordinated turn assumptions this algorithm reduces to a kinematics problem. In contrast to Berg's augmented adaptive jerk model, the prediction equation becomes non-linear, but does not require the explicit calculation of L, T, p, q, r. This algorithm can be simplified by assuming constant speed during the coordinated turn, which leads to a constant turn rate vector Ω [14, 15]. Nabaa and Bishop [16] have shown that the constant speed coordinated turn is a particular subset of the general coordinated turn of Bishop and Antoulas. In general the coordinated turn models are a set of non-linear, coupled equations, which are difficult to solve.

[*] Graduate Student, Department of Mechanical & Aerospace Engineering, State University of New York at Buffalo, Email: tenne@eng.buffalo.edu

[†] Associate Professor, Department of Mechanical & Aerospace Engineering, State University of New York at Buffalo, Email: tsingh@eng.buffalo.edu

Another geometric approach of implementing a circular turn has been introduced by Kawase et al. [17]. The circular prediction is constrained to lie on a circle which is defined from previous measurements, by calculating the center and the radius of the circle. The center-point-approach (CPA) predicts in a polar coordinate system (R and ψ) whose origin is the center of the circle. The CPA is not amenable for further stability, performance and uncertainty analysis, because of the complex center coordinate calculation and discontinuities in the polar angle ψ between successive scans. This discontinuity appears by switching from the previous circle to the current circle as the radius and center change.

In this work, the fact that a target trajectory has to be smooth even if the acceleration is impulsive is exploited to develop a new technique for target tracking. The proposed algorithm integrates the measured data into the filter and constrains the prediction to lie on a smooth curve, modeled, for example, by the arc of a circle. This filter algorithm becomes very flexible by readjusting the desired curve to account for maneuvering targets.

This paper proposes a new circular prediction algorithm in relative coordinates without the requirement of calculating the center and the radius. The predicted states are entirely defined in relation to the three points used to construct the circle. The proposed algorithm simplifies the prediction procedure and is amenable for further analysis. Furthermore, this filter algorithm becomes very flexible by readjusting the constraints for the predicted position to account for the behavior of the target trajectory, such that a coupling with the α-β filter becomes unnecessary. In the presence of uncertainties, the proposed filter can be aided by a dynamic scheduler for the states, to increase tracking performance.

2 The Circular Prediction Algorithm (static)

This section describes the filter algorithm where the target is assumed to travel on a circle with constant speed. The circle can be described by previous measurements and estimates of the target's position. In this paper we only use prior measurements to construct the circle.

To develop the algorithm, consider four points lying on a circle as shown in Figure 1(a). The four points are connected to create two triangles, $\triangle 123$ and $\triangle 134$ where the triangle sides are named by the points which they connect, for example R_{12} is the distance between points 1 and 2. The fourth point can be described relative to the points 1 to 3 by a variety of angle and distance combinations. A convenient pair is the angle φ_2 and the distance R_{34} as indicated in Figure 1(a). For targets with constant angular velocity R_{34} and φ_2 equal R_{23} and φ_1 respectively.

The desired prediction equations define the relationships between the fourth point, which is parameterized by R_{34} and φ_2 and the previous three points. To derive the prediction equation, consider the position of points 2, 3 and 4 relative to point 1, which is equivalent to introducing a Cartesian coordinate system labeled u-v with its origin at point 1 as shown in Figure 1(b). Equations 1a to 1d define the distances in terms of u_i and v_i.

$$R_{13}^2 = u_3^2 + v_3^2 \tag{1a}$$
$$R_{14}^2 = u_4^2 + v_4^2 \tag{1b}$$
$$R_{24}^2 = (u_4 - u_2)^2 + (v_4 - v_2)^2 \tag{1c}$$
$$R_{34}^2 = (u_4 - u_3)^2 + (v_4 - v_3)^2 \; . \tag{1d}$$

Equations 1c and 1d can be rewritten as:

$$u_2 u_4 + v_2 v_4 = R_{12} R_{14} \cos(\varphi_1 + \varphi_2) \tag{2a}$$
$$u_3 u_4 + v_3 v_4 = R_{13} R_{14} \cos(\varphi_2) \; . \tag{2b}$$

Solving Equations 2a and 2b for the relative position $[u_4 \; v_4]^T$, yields the desired relationship:

$$\begin{bmatrix} u_4 \\ v_4 \end{bmatrix} = \begin{bmatrix} u_2 & v_2 \\ u_3 & v_3 \end{bmatrix}^{-1} \begin{bmatrix} R_{12}\cos(\varphi_1 + \varphi_2) \\ R_{13}\cos(\varphi_2) \end{bmatrix} R_{14} \; . \tag{3}$$

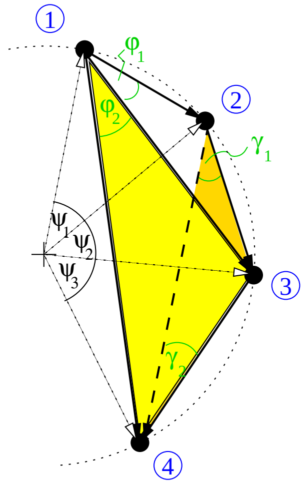

(a) Properties of four points lying on a circle

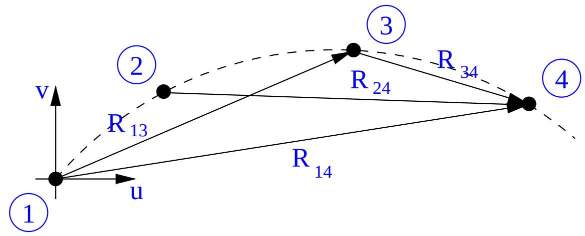

(b) Relative Relationships between four points on a circle

Figure 1: Properties of points lying on a circle

The unknown distance R_{14} in Equation 3 is determined from $\triangle 134$ using the cosine rule, in terms of the variables R_{34} and φ_2 as shown in Equation 4.

$$R_{14} = R_{13}\left[\cos(\varphi_2) \pm \sqrt{\left(\frac{R_{34}}{R_{13}}\right)^2 - \sin^2(\varphi_2)}\right] . \tag{4}$$

In case of a prediction with constant angular velocity ($\varphi_2 = \varphi_1$ and $R_{34} = R_{23}$) it can be shown that the smaller value of Equation 4 yields the trivial solution of $R_{14} = R_{12}$, and therefore the desired relationship for the prediction is the larger value. This equation is also valid for the non-constant angular velocity case since the smaller value of R_{14} would place the predicted position in the vicinity of point 2, which is not desirable.

The prediction Equations 3 and 4 exhibit a very general statement of predicting the fourth point in terms of the two state variables φ_2 and R_{34}. The assumption for the selection of these states defines the characteristics of the algorithm. The simplest approach for the prediction on a circle with constant angular velocity is achieved by choosing $\varphi_2 = \varphi_1$ and $R_{34} = R_{23}$. It becomes evident that scheduling the states φ_2 and R_{34} allow the filter to adjust to certain prediction properties, which is addressed in Section 3.

Some additional properties for points lying on a circle (Figure 1(a)), which will be necessary later in the paper, are listed below:

$$\varphi_2 = \gamma_1 \quad \text{and} \quad \varphi_1 = \gamma_2 \tag{5}$$

3 Dynamic Circular Filters

It is clear from Equations 3 and 5 that the estimation of the coordinates of the position of the target is only a function of φ_2 and R_{34}. Thus, different assumptions for the selection of φ_2 and R_{34} result in different filters. For instance, as was shown in the previous section, selecting $\varphi_2 = \varphi_1$ and $R_{34} = R_{23}$ results in an estimator which assumes that the target is moving with constant angular velocity on the arc of a circle. In the following section, other approaches to select φ_2 and R_{34} are proposed and their performances studied.

To account for noisy measurements, prediction information from the previous time step is used in the current time step. This makes the filter dynamic and permits the use of prior information to smooth out the noisy measurement data.

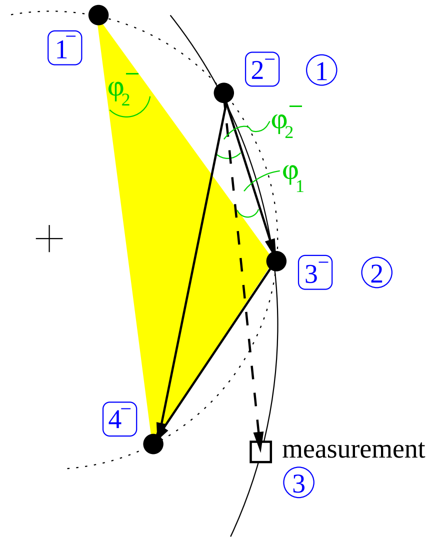

Figure 2: Estimation of the dynamic angle φ_2

3.1 Fixed Innovation Gain Filter

The first filter studied is where the selection of the angle φ_2 is a function of the predicted position and the measured position. Consider Figure 2 where point 4 on the circle represented by a dashed line, is the predicted position of the target. Now, a new measurement is received which is illustrated by a "□". To predict the next position of the target, unlike in the previous filter, the measured position is used in conjunction with the predicted position (point 4). The equation to fuse the measured position and the predicted position is

$$\varphi_2 = \varphi_2^- + k(\varphi_1 - \varphi_2^-) \ , \tag{6}$$

where φ_2^- is φ_2 from the previous time step, φ_1 is evaluated at the current time and k is a weighting factor, which when equal to one results in the constant angular velocity filter ($\varphi_2 = \varphi_1$) described in Section 2. This approach is motivated by the smoothing equation of the Kalman filter. Having selected φ_2, R_{34} is now determined so as to lie on a circle which passes through points 1, 2 and 3.

From the triangle $\triangle 234$ in Figure 1(a), the variable R_{34} can be calculated using the law of sines.

$$R_{34} = \frac{\sin(\gamma_1)}{\sin(\gamma_2)} R_{23} = \frac{\sin(\varphi_2)}{\sin(\varphi_1)} R_{23} \ , \tag{7}$$

where the relationship of equation 5 has been used.

With Equations 6 and 7, the dynamic circular prediction algorithm is complete. The predicted point is obtained by applying Equations 3 and 4 subsequently.

3.2 Dynamic Innovation Gain Filter

The weight in Equation 6 can be a constant or a time varying parameter. In the case of a constant gain filter, the difficulty in choosing a value, especially an optimal one arises. The task of optimal selection of the gain is naturally handled by the Kalman filter.

Designing a Kalman filter requires a dynamic model for the parameter φ_2. The dynamics are modeled as a stochastic acceleration process as shown in Equations 8.

$$\begin{bmatrix}\varphi_2\\ \omega_2\end{bmatrix}_{k+1} = \begin{bmatrix}1 & T\\ 0 & 1\end{bmatrix}\begin{bmatrix}\varphi_2\\ \omega_2\end{bmatrix}_k + \begin{bmatrix}\frac{1}{2}T^2\\ T\end{bmatrix} w_k \quad \Rightarrow \underline{\eta}_{k+1} = \Phi\underline{\eta}_k + \Gamma w_k \tag{8a}$$

$$z_k = \begin{bmatrix}1 & 0\end{bmatrix}\begin{bmatrix}\varphi_2\\ \omega_2\end{bmatrix}_k + v_k \quad \Rightarrow z_k = H\underline{\eta}_k + v_k, \tag{8b}$$

where the rate of change of the angle φ_2 is denoted by ω_2 and form together the state vector $\underline{\eta}$. Similar to Equation 6 we obtain the best estimate of the states $\underline{\eta}$ by choosing the innovation weight K as the Kalman gain. The Kalman filter loop is outlined as follows:

$$K_k = P_k^- H_k^T [H_k P_k^- H_k^T + R_k]^{-1} \tag{9a}$$

$$\hat{\underline{\eta}}_k = \underline{\eta}_k^- + K_k(\varphi_1 - H\underline{\eta}_k^-) \tag{9b}$$

$$P_k = (I - K_k H_k)P_k^- \tag{9c}$$

$$P_{k+1}^- = \Phi P_k \Phi^T + Q_k \tag{9d}$$

$$\hat{\underline{\eta}}_{k+1}^- = \Phi\hat{\underline{\eta}}_k\ . \tag{9e}$$

The matrices Φ, Γ and H are the transition, input and output matrices, respectively. Q and R are the process and measurement noise variances of the uncertainties w and v in Equations 8. The error covariance is denoted by P, where the superscript minus indicates the prior estimate.

One can find pathological trajectories when the circular filter would perform poorly. One such example is when the target transitions from a circular trajectory to a straight line. Since the update relationship (Equation 6 or 9b) uses a small φ_1 and a large φ_2^-, it results in a large prediction error. Thus, there is a motivation for integrating the circular filter with a filter, which works efficiently for straight line trajectories such as an α-β, or α-β-γ filter.

4 Hybrid Filters

The prediction algorithms developed in Sections 2 and 3 are reasonable for circle like trajectories. However, real trajectories can be approximated by piecewise curves which are circles and straight lines, and therefore the performance of a stand alone circular filter would degrade. The proposed circular filters are therefore integrated with traditional filters, such as fixed parameter α-β filters. These hybrid filters improve the tracking performance for a variety of maneuvers.

The circular prediction algorithm defined in Section 2 is referred to as the *static* circular prediction and the algorithm described in Section 3 is referred to as the *dynamic* circular prediction, where the dynamic prediction is further classified by the innovation gain. These three circular prediction algorithms are combined with direction decoupled α-β filters to form hybrid filters. The equations of the α-β filter are

$$x_p(k+1) = x_s(k) + Tv_s(k) \tag{10a}$$

$$x_s(k) = x_p(k) + \alpha(x_o(k) - x_p(k)) \tag{10b}$$

$$v_s(k) = v_s(k-1) + \frac{\beta}{T}(x_o(k) - x_p(k))\ , \tag{10c}$$

where x_o and x_p are the measurement and the prediction respectively. The sampling time is denoted by T and the innovation gains are α for the position and β for the velocity equation.

The prediction of the circular filter and the α-β filter are fused by a weighting scheme proposed by Kawase et al. [17]. The weight is defined by the prediction error of each filter at time step k and is used in the prediction for the next time step $k+1$. The weight is calculated as:

$$w_k = \left.\frac{e_{\alpha\beta}}{e_{\alpha\beta} + e_{\text{circle}}}\right|_k\ , \tag{11}$$

where the error is defined as the distance of the previous prediction and the measurement:

$$e_k = |\vec{x}_p - \vec{x}_o|_k \ . \tag{12}$$

The value of the weight lies in the interval [0 1], where a perfect match of the α-β prediction with the measurement ($e_{\alpha\beta} = 0$) yields a vanishing weight and in the case of $e_{\text{circle}} = 0$, the weight becomes one. The combined prediction is therefore defined as:

$$\vec{x}_p(k+1) = (1 - w_k)\vec{x}_{p\alpha\beta} + w_k \vec{x}_{\text{circle}} \ . \tag{13}$$

Summarizing the aforementioned algorithms yields the following list of tracking filters.

Stand alone Filters	Filter 1 Fixed gain α-β filter
	Filter 2 Static circular prediction
	Filter 3 Dynamic circular prediction with constant innovation gain k
	Filter 4 Dynamic circular prediction with Kalman innovation gain K
Hybrid Filters	Filter 5 α-β filter combined with Filter 2
	Filter 6 α-β filter combined with Filter 3
	Filter 7 α-β filter combined with Filter 4

These filter labels are used in the performance section for brevity.

5 Tracking Performance

Benchmark tests are carried out to compare the performance of the filters. The tests are performed on the target trackers listed in the previous section. Motivated by the inherent tracking capability of each filter, three trajectories have been chosen as benchmark trajectories. These are constant velocity and constant acceleration circular trajectories and non-maneuvering targets moving on a straight line.

5.1 Targets with constant angular velocity on a Circular Trajectory

Figure 3(a) shows a target on a circular trajectory denoted by the dashed line. The measurements of successive scans are displayed as squares "□", which were generated using process noise in a Cartesian system to simulate uncertainties in the model and measurement noise in a polar system to reflect range-bearing sensors. The root-mean-square (rms) value of the prediction errors of the seven filters are listed in Table 1.

Filter	Single Filters				Combined Filters		
	1	2	3	4	5	6	7
Mean value $[m]$	303.84	**249.27**	289.07	252.93	**229.29**	239.75	230.52
Variance $[m^2]$	203.91	1124.30	20866.12	1587.76	540.29	3377.18	619.47

Table 1: Mean and variance of the rms value of the prediction errors for a target with constant angular velocity on a circular trajectory

The performed test shows that combining the circular prediction with the α-β filter decreases the prediction error. This fact is attributed to the additional noise smoothing capability of the α-β filter. On the contrary, the single α-β filter poorly predicts the target on the circle because it lacks the ability to predict accelerating targets. Figure 3(a) shows an increasing off-set in the predicted trajectory of the α-β filter, whereas the circular predictions track the circular path of the target.

The static circular predictor (Filter 2) exhibits a reasonable performance since the target travels with constant angular velocity. The uncertainties in the measurement and the process noise increase the prediction error. The tracking performance of the dynamic filters is comparable to the static algorithm. The performance depends on the choice of the parameters, the innovation gain of the Filter 3 and 6 and on the measurement and process noise variances of the Kalman filter (Filters 4 and 7). In addition, the decreased performance of the Kalman filter is a result of modeling the acceleration as process noise.

This example trajectory also illustrates situations in which the circular filters result in chatter in the tracking performance. If the circle created by the measurements has a curvature which is opposite of that of the true trajectory, due to measurement noise, the predictions begin to chatter around the true target position. This is shown in Figure 3(a) in the bearing range of 135° to 225°.

5.2 Targets with constant acceleration on a circular trajectory

Figure 3(b) shows a target traveling with constant angular acceleration along a circular path. The prediction errors for this maneuver are listed in Table 2.

Filter	Single Filters				Combined Filters		
	1	2	3	4	5	6	7
Mean value $[m]$	771.30	251.99	262.15	**251.67**	283.24	285.69	**282.94**
Variance $[m^2]$	362.73	1416.16	2328.34	1454.14	1292.50	1164.36	1288.09

Table 2: Mean and variance of the rms value of the prediction errors for a target with constant angular acceleration on a circular trajectory

The prediction error of the α-β filter increased significantly compared to the constant angular velocity target listed in Table 1. Similarly, the α-β filter prediction exhibits an off-set from the targets actual circle. In contrast, the circular filters follow the contour of the target's trajectory. Observing the prediction error results, reveal that combining the circular predictions with an α-β filter decrease the prediction performance. The weighting scheme could be responsible for the decreased performance and needs to be improved in further studies. Since the target is accelerating, the circular prediction involving the Kalman filter exhibits the smallest prediction error. These filters (Filter 4 and 7) are the only filters modeling the acceleration.

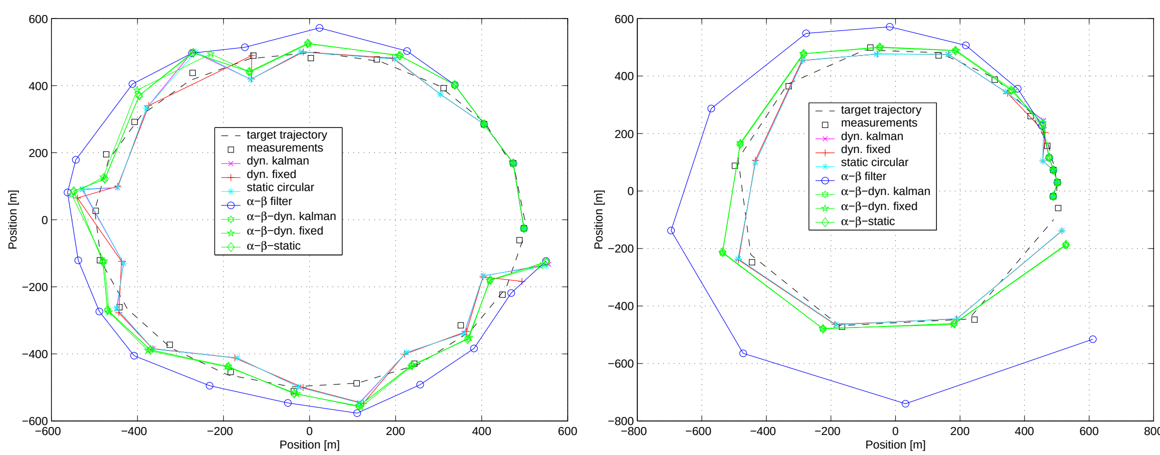

(a) Non-accelerating target ($\omega = 0.005141$/s, $R =$ 500m, sampling Time = 60s, 20 scans)

(b) Accelerating target ($\omega_0 = 0$, $\dot{\omega} = 2 \cdot 10^{-5} 1/s^2$, $R = 500$m, sampling Time = 60s, 13 scans)

Figure 3: Targets on a circular trajectory

5.3 Non-maneuvering Targets on a Straight Line

The final benchmark test is a straight line trajectory with a target traveling at constant speed of 3 knots. This target motion is preferred by the α-β filter and Table 3 shows the lowest prediction error for the α-β filter. The circular predictions (Filters 2 to 4) exhibit a relatively high prediction error, but the combination with an α-β filter improves the prediction performance significantly.

Filter	Single Filters				Combined Filters		
	1	2	3	4	5	6	7
Mean value $[m]$	**106.00**	208.33	220.90	209.52	**136.77**	135.96	137.01
Variance $[m^2]$	492.36	2382.95	4159.74	2358.00	862.69	951.92	849.15

Table 3: Mean and variance of the rms value of the prediction errors for a non-maneuvering target on a straight line

6 Summary

A simple circular prediction scheme has been developed and it has been shown that this algorithm combined with an α-β filter significantly improves the prediction performance for both curved and straight line maneuvers.

Since, the proposed approach of predicting the target position on an arc of a circle does not require any if-then logic statements, it is simpler than that proposed in the literature. This also permits further analysis related to stability and performance. The formulation of the circular filter in the setting of an Extended Kalman filter will be carried out in the future. Knowledge of the process noise and measurement noise can be used to arrive at an optimal circular filter.

Finally, the fusion of the two filters, an α-β filter and a circular prediction algorithm, reveal a significant improvement in the tracking performance. Inclusion of an α-β-γ filter can improve the tracking performance further, by being able to track targets accelerating on straight lines.

References

[1] Jack Sklansky. Optimizing the dynamic parameter of a track-while-scan system. *RCA Laboratories, Princton, N.J.*, June 1957.

[2] T. R. Benedict and G. W. Bordner. Synthesis of an optimal set of radar track-while-scan smoothing equations. In *IRE Transactions on Automatic Control*, volume AC-1, July 1962.

[3] Paul R. Kalata. $\alpha - \beta$ target tracking systems: A survey. In *American Control Conference/WM12*. ECE Department, Drexel University Philadelphia, Pennsylvania, 1992.

[4] H. R. Simpson. Performance measures and optimization condition for a third order sampled-data tracker. In *IEEE Transactions on Automatic Control*, volume AC-12, June 1962.

[5] Paul R. Kalata. The tracking index: A generalized parameter for $\alpha - \beta$ and $\alpha - \beta - \gamma$ target trackers. In *IEEE Transactions on Aerospace and Electronic Systems*, volume AES-20, No.2. ECE Department, Drexel University Philadelphia, Pennsylvania, March 1984.

[6] Yaakov Bar-Shalom and Thomas E. Fortmann. *Tracking Data and Association.* Academic Press, Inc., 1988.

[7] John A. Lawton, Robert J. Jesionowski, and Paul Zarchan. Comparison of four filtering options for radar tracking problem. *Journal of Guidance, Control and Dynamics*, 21(4), July-August 1998.

[8] A.T. Alouani, P. Xia, T.R. Rice, and W.D. Blair. A two-stage Kalman Estimator for tracking Maneuvering targets. *Proceedings of the IEEE International Conference on Systems, Man, and Cybernetics*, 2, 1991.

[9] R. A. Singer. Estimating optimal tracking filter performance for manned maneuvering targets. In *IEEE Transactions on Aerospace and Electronic System*, volume AES-5, November 1970.

[10] Russell F. Berg. Estimation and prediction for maneuvering target trajectories. In *IEEE Transaction on Automatic Control*, volume AC-28, pages 294–304, March 1983.

[11] R. von Mises. *Theory of Flight*. McGraw-Hill Book Co., New York, 1945.

[12] R. H. Bishop and A. C. Antoulas. Non-linear approach to the aircraft tracking problem. In *Proceedings of the 1991 AIAA Guidance, Navigation and Control Conference*, volume 1, pages 692–703, New Orleans, LA, August 1991.

[13] R. H. Bishop and A. C. Antoulas. Non-linear approach to the aircraft tracking problem. *Journal of Guidance, Control and Dynamics*, 17(5):1124–1130, September–October 1994.

[14] S. Blackman and R. Popoli. *Design Analysis of Modern Tracking Systems*. Artech House, Norwood, MA, 1999.

[15] T.E. Bullock and S. Sangsuk-Iam. Maneuver detection and tracking with a noonlinear target model. In *Proceedings of the 23rd Conference on Decision and Control*, volume 1, pages 1122–1126, Las Vegas, NV, December 1984.

[16] N. Nabaa and R. H. Bishop. Validation and comparison of coordinated turn aircraft maneuver models. In *IEEE Transaction on Aerospace and Electronic Systems*, volume 36, pages 250–259, January 2000.

[17] T. Kawase, K. Tsarunosono, N. Ehara, and I. Sasase. An adaptive-gain alpha-beta tracker combined with circular prediction for maneuvering target tracking. In *IEEE TENCON - Speech and Image Technologies For Computing and Telecommunications*, 1997.